Int. J. Heat Mass Transfer. Vol. 13, pp. 383–393. Pergamon Press 1970. Printed in Great Britain

CALCULATION OF VOID VOLUME FRACTION IN THE SUBCOOLED AND QUALITY BOILING REGIONS

S. Z. ROUHANI* and E. AXELSSON†
Aktiebolaget Atomenergi, Stockholm, Sweden

(*Received* 10 *January* 1969 *and in revised form* 1 *July* 1969)

Abstract—The complex problem of void calculation in the different regions of flow boiling is divided in two parts.

The first part includes only the description of the mechanisms and the calculation of the rates of heat transfer for vapour and liquid. It is assumed that heat is removed by vapour generation, heating of the liquid that replaces the detached bubbles, and in some parts, by single phase heat transfer. By considering the rate of vapour condensation in liquid, an equation for the differential changes in the true steam quality throughout the boiling regions is obtained. Integration of this equation yields the vapour weight fraction at any position.

The second part of the problem concerns the determination of the void fractions corresponding to the calculated steam qualities. For this purpose we use the derivations of Zuber and Findlay [9].

This model is compared with data from different geometries including small rectangular channels and large rod bundles. The data covered pressures from 19 to 138 bars, heat fluxes from 18 to 120 W/cm^2 with many different subcoolings and mass velocities. The agreement is generally very good.

NOMENCLATURE

a, a dimensional constant in equation (16) [m$^{-\frac{1}{4}}$];
a_1, a dimensional constant in equation (12) [m$^{-\frac{1}{4}}$];
a_2, a proportionality constant in equation (15);
A_b, contact area between the bubbles and the liquid per unit length of the channel [m^2];
A_c, flow area in the channel [m^2];
C, distribution parameter in equation (8);
C_p, specific heat of liquid at constant pressure [J/kg°C];
D_e, equivalent hydraulic diameter, $4A_c/P_t$ [m];
G, mass velocity [kg/m^{2}s];
h, heat transfer coefficient (Collburn's correlation) [W/m^2°C];
k_c, condensation factor [W/m°C];
k_l, thermal conductivity of liquid [W/m°C];
$\dot{m}$, total mass flow rate [kg/s];
$\dot{m}_s$, mass of liquid which is converted into steam per unit time per unit area of the heated surface [kg/m^{2}s];
N_q, a dimensionless number defined by equation (14);
p, pressure [N/m^2];
P_h, heated perimeter [m];
Pr, Prandtl number $C_p\mu_l/k_l$;
q/A, heat flux [W/m^2];
Q_b, the amount of heat which is absorbed by boiling per unit time per unit length of channel [W/m];
Q_c, the amount of heat which is exchanged by condensation of bubbles per unit time per unit length of channel [W/m];
Re, Reynolds number, $G \cdot De/\mu$;
t_l, liquid temperature in the presence of steam flow [°C];
t_s, saturation temperature [°C];
x, true vapour weight fraction (steam quality);

* Section for Thermal Design of Reactors.
† Section for Applied Mathematics.

x_0, average steam quality;
z, distance along the heated channel measured from the inlet [m];
α, vapour volume fraction (void);
α_c, upper limit of wall voidage given by equation (1);
θ_l, liquid subcooling as an integral of equation (9), $t_s - t_l$ [°C];
θ_0, average liquid subcooling obtained from a heat balance for the whole flow [°C];
$\varepsilon(p)$, a pressure-dependent non-dimensional parameter defined in equation (15);
λ, latent heat of vaporization [J/kg];
μ_l, dynamic viscosity of liquid [kg/m s];
ρ_g, vapour density [kg/m^3];
ρ_l, liquid density [kg/m^3];
σ, surface tension of liquid [N/m].

1. INTRODUCTION

THE CALCULATION of void in subcooled flow boiling is particularly complex because of the absence of thermal equilibrium between the two phases. For this reason the problem of subcooled void calculation must be divided in two parts:

1. A close estimation of the true liquid subcooling and the vapour weight fraction at any position,
2. The determination of the vapour volume fraction for the calculated steam qualities in the given conditions.

A particular approach to the solution of these problems was described in a previous report [1].

The method of void calculation suggested in [1] was only applicable to the regions of subcooled boiling and was approximative regarding the influence of slip velocity.

The main improvement in the present model over that of [1] is the admission of slip velocity between vapour and liquid even in the region of subcooled boiling. The inclusion of a slip ratio other than unity in this model improves it considerably and makes it applicable to a wider range of conditions. The present model is valid even in the net boiling region.

Another improvement is the inclusion of a unified correlation for the condensation constant throughout the regions of subcooled boiling. This eliminates any discontiuity in transitions between the different boiling regions.

2. LITERATURE SURVEY

A literature survey on the papers dealing with the calculation of void fraction in subcooled boiling was given in [1]. The survey included works of Griffith *et al.* [2], Maurer [3], Bowring [4], Costello [5] and Delayre and Lavinge [6].

Several additional reports on this subject have appeared in the literature recently. Among these are the works of Levy [7] and Zuber *et al.* [8].

The main points of the paper by Levy [7] is a new method of calculating the liquid subcooling at the point of bubble departure. This is different from Bowring's method [4]. Levy suggests also a certain relationship between the true local vapour weight fraction and the corresponding thermal equilibrium value. Finally, by applying an accepted slip correlation he calculates the void fraction in subcooled boiling.

Zuber *et al.* [8] emphasize the influence of flow regime upon the relative vapour velocity throughout the boiling regions. With the inclusion of a concentration constant and the drift velocity of the bubbles as presented in [9] they give a better description of the average slip velocity. For the particular region of subcooled boiling they assume a mathematically feasible function for liquid temperature distribution along the heated channels. They apply Bowring's correlations [4] to determine the location of bubble detachment and finally, in the absence of a method of predicting the limits of various flow regimes, they make use of a fixed value of concentration constant for all conditions.

3. THEORY

3.1 *Basic assumptions*

As explained in the introduction one should

first estimate the true vapour weight fraction at any position along the channel. This may be done through proper heat balance equations for each phase in axial and transverse directions in the channel.

We consider first the transverse heat flow from the heated surface to the boiling flow. The assumed mechanisms of heat removal in this model are the same as given in [1]. These are briefly repeated below:

1. Single phase heat transfer which will be partially effective as long as the heated surface is not covered with bubbles,
2. Steam generation,
3. Heating of that mass of water which replaces the detached bubbles.

At least two of these mechanisms are effective in parallel on the heated surface while some heat exchange between steam bubbles and the subcooled liquid will take place through condensation.

3.2 *The separate regions of subcooled boiling*

As pointed out in many reports on the subject of subcooled boiling [1–8] there exists a certain limit of subcooling at which the bubbles begin to detach from the heated wall. It is assumed that the bubbles generated at subcoolings larger than that of the point of detachment are mostly stationary and collapse before moving away from the wall. The void fraction due to the stationary bubbles is termed wall voidage and it has an upper limit which depends on pressure, heated perimeter and the flow area.

According to the works of Maurer [3], Bowring [4] and Costello [5], and as explained in [1], we consider two regions of subcooled boiling:

1. Local boiling with stationary bubbles on the surface and high subcooling,
2. Local boiling with low enough subcooling to allow bubble detachment and flow of vapour bubbles with liquid.

The maximum value of wall voidage occurs at the end of the first region. We refer to the void fraction at the end of the first region by α_c. The basis of calculation of α_c was explained in [1] and it was concluded that for water as the boiling medium

$$\alpha_c = 2{\cdot}435 \cdot 10^{-3}\, p^{-0{\cdot}237} \frac{P_h}{A_c}. \qquad (1)$$

In this equation p is in N/m^2, P_h in m and A_c in m^2.

The second region starts at the point of detachment and ends at a position where the liquid subcooling becomes negligible.

3.3 *Derivation of the basic equations*

We assume that local boiling starts at a point where

$$\frac{q}{A} - h(t_s - t_l) > 0 \qquad (2)$$

h is the single phase heat-transfer coefficient for only liquid flow.

We use Collburn's correlation which gives

$$h = \frac{0{\cdot}023}{Re^{0{\cdot}2}} G \cdot C_p \cdot Pr^{-\frac{2}{3}}. \qquad (3)$$

At high subcoolings the single phase heat transfer will still be effective but accompanied by the other mechanisms. As the subcooling decreases the heated surface will become more and more covered with bubbles and hence less accessible to the bulk liquid flow. For this reason we assume that the non-boiling fraction of heat flux will be

$$\left(\frac{q}{A}\right)_{nb} = \left(1 - \frac{\alpha}{\alpha_c}\right) h(t_s - t_l) \quad \text{for } \alpha < \alpha_c \qquad (4)$$

in which α is the local void fraction and α_c is the void fraction at the point of vapour clotting.

The non-boiling fraction of heat flux will gradually decrease with increasing wall voidage and it vanishes when the wall voidage reaches α_c.

The heat balance on the heated surface is

$$\frac{q}{A} = h\theta_l \left(1 - \frac{\alpha}{\alpha_c}\right) + \dot{m}_s \cdot \lambda + \frac{\dot{m}_s}{\rho_g} C_p \cdot \rho_l \cdot \theta_l \qquad (5)$$

For values of α larger than α_c, the first term on the right-hand side of this equation should be eliminated.

The amount of heat which goes to steam generation per unit time within dz along the channel will be

$$dQ_b = \dot{m}_s \lambda P_h \cdot dz = \frac{(q/A) - h\theta_l[1 - (\alpha/\alpha_c)]}{\rho_g \cdot \lambda + C_p \rho_l \theta_l} \rho_g \lambda P_h \, dz. \quad (6)$$

Again for $\alpha > \alpha_c$ the term containing h must be eliminated.

The amount of heat which goes to the subcooled liquid through condensation of vapour bubbles per unit time within dz may be expressed as

$$dQ_c = k_c \cdot \theta_l \, dz \quad (7)$$

in which k_c is a condensation coefficient with the same dimensions as that of the thermal conductivity. It will be shown that this constant is actually proportional to the thermal conductivity of the liquid phase divided by the Prandtl number.

Considering the heat balance in the axial direction we use two separate equations for the two phases. The connection between the two heat balance equations is found in equation (7) which gives the rate of heat exchange between vapour and liquid.

Without making any distinction between the different regions of boiling, one may write the heat balance for the vapour phase within dz as

$$dx = \frac{dQ_b - dQ_c}{\dot{m} \cdot \lambda}. \quad (8)$$

This is the differential change in the true vapour fraction with dz regardless of the flow regime or slip ratio.

The total heat balance across dz gives the differential change in the true liquid subcooling as

$$d\theta_l = \frac{(q/A) \cdot P_h \cdot dz - (dQ_b - dQ_c)}{\dot{m} \cdot C_p}. \quad (9)$$

Now, assuming that the variations of dQ_b and dQ_c with z are known, one may integrate equation (8) to obtain the true steam quality at any height.

With the known values of steam quality x, one may use a suitable relationship for slip ratio and calculate the local values of the void volume fraction.

It will be shown that k_c is dependent on the local void fraction in a non-linear manner. For this reason dx in equation (8) becomes a non-linear function of z and therefore it may only be integrated by numerical methods.

For the calculation of the average local void from steam quality, the authors draw upon the derivations of Zuber and Findlay [9] and use the following relation:

$$\alpha = \frac{x}{\rho_g}\left\{C\left[\frac{x}{\rho_g} + \frac{1-x}{\rho_l}\right] + \frac{1{\cdot}18}{G} \times \left[\frac{\sigma \cdot g(\rho_l - \rho_g)}{\rho_l^2}\right]^{\frac{1}{4}}\right\}^{-1}. \quad (10)$$

In this equation, C is a distribution parameter which is dependent on the velocity profile and void distribution over flow area.

Although one would expect that C should vary with channel geometry and flow regimes, we have found that an average value of about 1·1 would be adequate to match the data from a large variety of test geometries. However, a rather strong dependence of C upon the mass velocity was observed for the lower values of the latter parameter ($G < 200$). For low velocities C was found to be much larger than 1·1.

4. ESTIMATION OF THE RATE OF BUBBLE CONDENSATION

The condensation coefficient, k_c, in equation (7) is dependent on many parameters. Physically, this coefficient must depend on the thermal conductivity of the liquid and some other properties of the two phases. It must be a function of the local values of contact area between vapour and liquid which is to some extent dependent on the void fraction and the

channel geometry. Finally, mass velocity and heat flux must have some influence upon the condensation parameter.

The individual effects of these parameters were determined by a systematic comparison of this model with the data of [10] in a manner explained in the Appendix. The general validity of the model and the related dependencies upon various parameters were then verified by comparing this calculation procedure with a large number of data from different sources [11–14].

4.1 *Selection of the distribution parameter*

Before any studies on the effects of different parameters upon k_c the data of net boiling regions were used in equation (10) to obtain a suitable value of C. In most cases the average value of this parameter turned out to be

$$C = 1{\cdot}12. \tag{11a}$$

This value of the distribution parameter was then used in equation (10) for the region of subcooled boiling.

For the case of low mass velocities of [10] it was found that

$$C = 1{\cdot}54. \tag{11b}$$

4.2 *Effect of void and channel geometry on* k_c

As described in [1] the average contact area between the bubbles and liquid may be expressed as

$$A_b = a_1 \cdot A_c^{\frac{1}{2}} \cdot \alpha^{\frac{1}{2}} \quad \text{(per unit length)} \tag{12}$$

in which a_1 is a proportionality constant which may depend on the heat flux (bubble generation frequency).

4.3 *Effect of mass velocity and heat flux*

The effect of mass velocity is included in a non-dimensional form by using Reynolds number calculated for the local liquid velocity

$$(Re)_l = \frac{G \cdot De}{(1 - \alpha)\mu_l}. \tag{13}$$

A systematic comparison with the experimental data of [10] showed that the condensation coefficient varied linearly with $(Re)_l$. This equation illustrates another dependence of k_c upon α. The effect of heat flux is also included in a non-dimensional manner by using the following dimensionless number: (see Appendix)

$$N_q = \frac{(q/A)\mu_l}{\lambda(\rho_l - \rho_g)\sigma}. \tag{14}$$

The dependence of k_c on N_q was found to be as $1/\sqrt{N_q}$.

4.4 *Effect of physical properties on* k_c

Apart from the effect of physical properties through $(Re)_l$ and N_q, it was seen that k_c varied with pressure considerably with all the other parameters being the same. The effect of pressure could be represented with the following group of parameters (see Appendix)

$$\varepsilon(p) = a_2 \frac{k_l}{Pr}\left(\frac{\rho_g}{\rho_l}\right)^2 \quad \text{for} \quad p \geqslant 19b \tag{15}$$

in which a_2 is a dimensionless constant.

4.5 *The proposed correlation for the condensation parameter*

Based on the above mentioned results it was found that

$$k_c = a \cdot \frac{k_l}{Pr}\left(\frac{\rho_g}{\rho_l}\right)^2 A_c^{\frac{1}{2}} \cdot \alpha^{\frac{1}{2}} \cdot (Re)_l / N_q^{0{\cdot}5} \tag{16}$$

in which $a = a_1 \cdot a_2 = 30{\cdot}0\ \mathrm{m}^{-\frac{1}{2}}$ is a dimensional constant and may probably depend on the number of nucleation sites per unit area of the heated surface as well as on the bubbling frequency and other factors.

Equation (16) is applicable in both regions of subcooled boiling.

5. COMPARISON WITH DATA UNDER VARIOUS CONDITIONS

The general validity of the model and the related dependencies upon various parameters were verified by comparing this calculation

Table 1. Range of data used in comparison with this model

Source of data	Test section: Geometry	Flow area (cm^2)	Heated perimeter (cm)	Pressure (bar)	q/A (W/cm^2)	G ($kg/m^2.s$)	θ (°C)	x (%)
Ref. [10]	annular	3·78	3·77	19–50	60–120	130–1450	0–130	0–12
Ref. [11]	6-rod cluster	30·5	26·2	31·6–51·4	46·7–64·5	1345–1607	5·7–27·2 (corrected)	0–6
Ref. [12]	36-rod cluster	142·7	156·0	50·0	22–64	1110–1159	11–22·4	2–9
Ref. [13]	rectangular 1·11 × 4·44 cm	4·93	11·1	51·0–69·9	49·6	877–906	12·5	6–7
Ref. [14]	rectangular 0·261 × 2·54	0·665	5·6	137·9	18·9–0 126·1	9080–1165	5–73·4	8–18

procedure with a large number of data from different geometries obtained over a wide range of parameters.

Table 1 gives a brief description of the test geometries and the range of parameters covered.

The void volume fraction corresponding to the experimental conditions were computed by

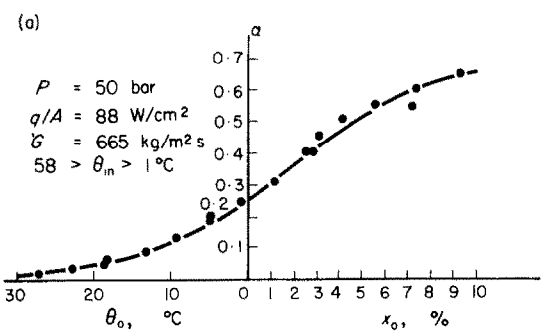

FIG. 1(a). Comparison of this model with data of Ref. [10]. Annular test section, low mass velocity.

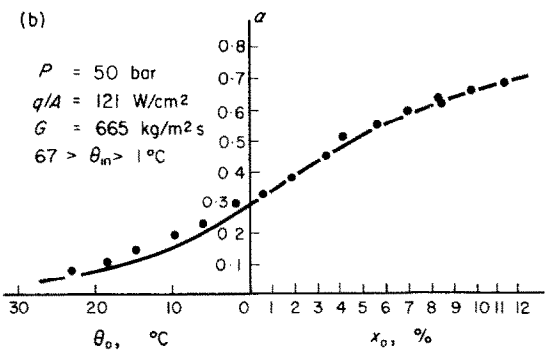

FIG. 1(b). Comparison with data of Ref. [10]. High heat flux, low mass velocity.

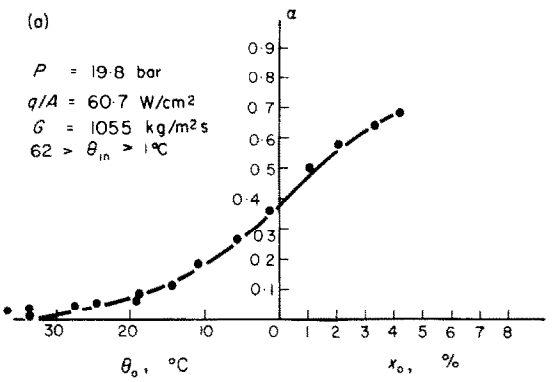

FIG. 2(a). Comparison with data of Ref. [10]. Low heat flux.

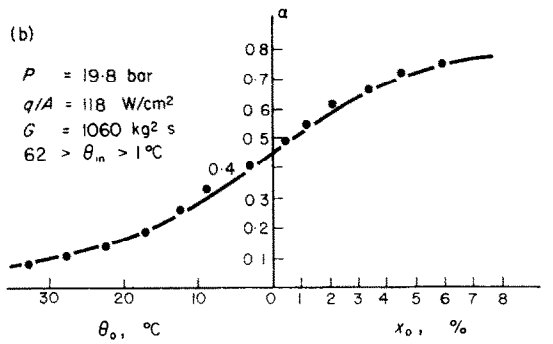

FIG. 2(b). Comparison with data of Ref. [10]. High heat flux.

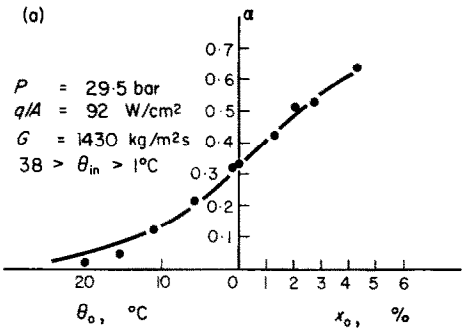

FIG. 3(a). Comparison with data from annular test section [10].

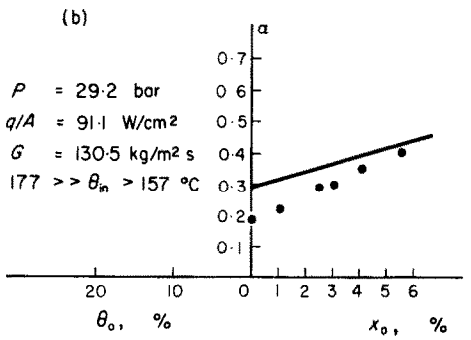

FIG. 3(b). Comparison with data from annular test section [10]. Very low mass velocity.

numerical integration of equations (6)–(9) and using equations (1), (3), (10) and (16).

Graphical comparisons of the results of computations with experimental data are shown in Figs. 1–7.

For the case of data of [10] in which voids are given at a fixed position in the channel at 109 cm from the inlet, the comparisons are made by plotting voids as a function of the local average subcooling or local average steam quality. These average values are calculated by assuming thermal equilibrium in the channel and neglecting the true vapour flow. These are good only as some reference points for comparison. The true liquid subcoolings calculated from equation (9) are considerably different from average subcoolings, θ_0. Likewise, the lower values of the average steam quality are considerably different from the true steam qualities obtained from equation (8).

As can be seen in Fig. 3(b) the agreement between the model and data with very low mass velocities ($G = 130$ kg/m^2 s) is rather poor for very large inlet subcooling ($\theta_{in} > 150$°C). It has not been possible to find out whether this discrepancy depends on the effect of mass velocity, on the rate of condensation, or on the effect of variations of physical properties because of the large temperature variations.

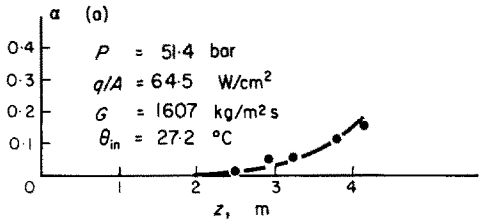

FIG. 4(a). Comparison with measurements in a 6-rod cluster (Run No. 13028 of Ref. [11]).

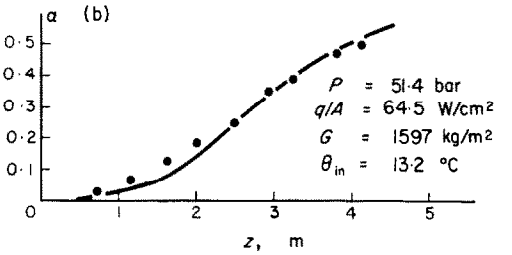

FIG. 4(b). Comparison with measurements in a 6-rod cluster (Run No. 13027 of Ref. [11]).

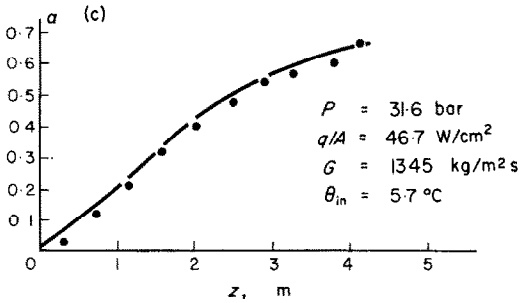

FIG. 4(c). Comparison with measurements in a 6-rod cluster (Run No. 13026 of Ref. [11]).

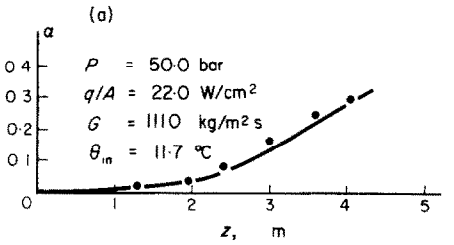

FIG. 5(a). Comparison with measurements in a 36-rod cluster (Run No. 313007 of Ref. [12]).

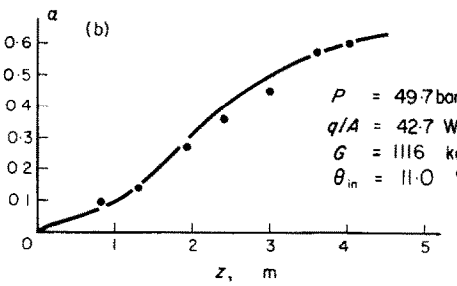

FIG. 5(b). Comparison with measurements in a 36-rod cluster (Run No. 313015 of Ref. [12]).

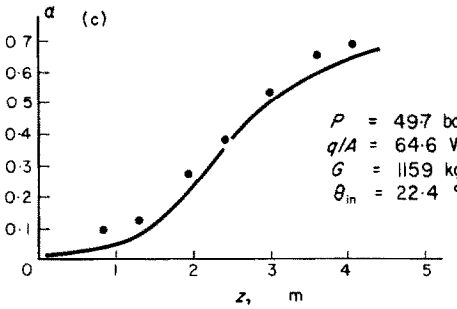

FIG. 5(c). Comparison with measurements in a 36-rod cluster (Run No. 313020 of Ref. [12]).

Although the effect of natural convection on the single-phase heat transfer has been considered, it is plausible that in the presence of steam bubbles near the inner surface of the annular geometry there has been some sort of intensified convection at very low mass velocities. Heat removal through such mechanisms has not been accounted for in these calculations.

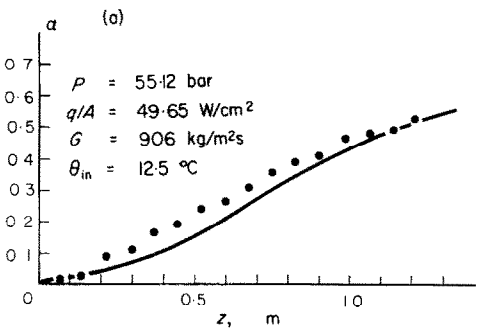

FIG. 6(a). Comparison of this model with Christensen's data [13]. Rectangular test section.

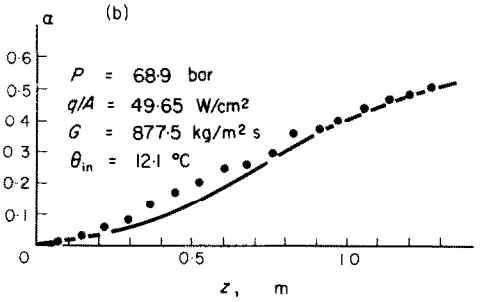

FIG. 6(b). Comparison of this model with Christensen's data [13]. Rectangular test section.

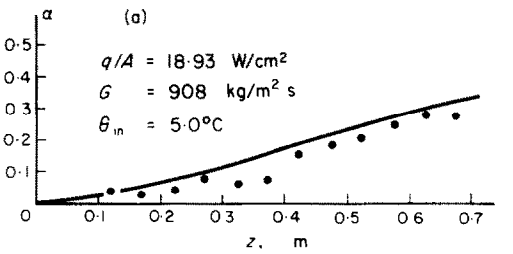

FIG. 7(a). Comparison with the data of BMI at 138 bars (Condition No. 11 of Ref. [14]).

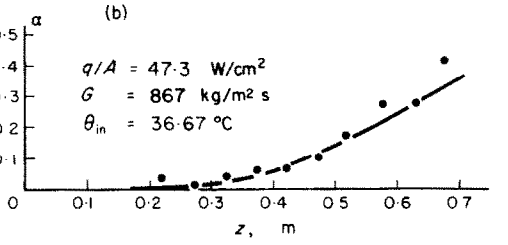

FIG. 7(b). Comparison with the data of BMI at 138 bars (Condition No. 6 of Ref. [14]).

Figures 1(a)–3(a) show very good agreement between the calculation and the data under different conditions. These are only samples of many similar tests of this model against the data of [10].

Figures 4 and 5 show the comparisons with data from rod bundles with six and thirty six rods respectively [11, 12]. The calculated voids match the data quite well.

Comparisons with the data from two rectangular geometries are shown in Figs. 6 and 7. These include runs at pressures up to about 140 atm. The largest deviation (in the case of Christensen's data at 56 atm) seems to be about 6 per cent void. The admitted limits of experimental errors for these data are ± 5 per cent.

The computed voids for the conditions of data from Battelle Memorial Institute [14] are shown in Figs. 7(a) and 7(b). On the average the computed results show good agreement even with the data from these experiments.

6. CONCLUSIONS

Based on the results of comparison with the experimental data it may be concluded that the present model gives a very close approximation of the true physical phenomena involved in the changes of steam volume fraction in flow boiling throughout the boiling regions.

In the absence of data from subcooled boiling of other liquids, nothing can be said on the applicability of the correlation for the condensation factor in general. However, it seems to agree quite well with the properties of water and heavy water for pressures from 19 to 140 atm.

REFERENCES

1. S. Z. ROUHANI, Calculation of steam volume fraction in subcooled boiling, *J. Heat Transfer* **90**, 158–164 (1968).
2. P. GRIFFITH, I. A. CLARK and W. M. ROHSENOW, Void volumes in subcooled boiling systems, ASME 58-HT-19 (1958).
3. G. W. MAURER, A method of predicting steady-state boiling vapour fractions in reactor coolant channels, WAPD-BT-19 (1960).
4. R. W. BOWRING, Physical model, based on bubble detachment and calculations of steam voidage in subcooled region of a heated channel, HPR 10 (1962).
5. C. P. COSTELLO, Aspects of local boiling effects on density and pressure drop, ASME 59-HT-18 (1959).
6. R. DELAYRE and P. LAVIGNE, Friction pressure drop for flow of boiling water at high pressure appendix—model of void fraction, *EAES Symp. on Two-Phase Flow and Steady State Burnout and Hydraulic Instability*, October 1st–3rd, Vol. 1 AB Atomenergi, Studsvik, Sweden (1963).
7. S. LEVY, Forced convection subcooled boiling-prediction of vapour volumetric fraction, GEAP-5157 April (1966).
8. N. ZUBER, F. W. STAUB and G. BIJWAARD, Vapour void fraction in subcooled boiling and in saturated boiling systems, III *International Heat Transfer Conference*, ASME-153 (1966).
9. N. ZUBER and J. FINDLAY, Average volumetric concentration in two-phase flow systems, *J. Heat Transfer* **87**, Ser. C, 453–462 (1965).
10. S. Z. ROUHANI, Void measurements in the region of subcooled and low quality boiling, Part 2, AE-239 (1966).
11. G. EKLUND, O. GELIUS and O. NYLUND, FRÖJA, FT-6 preliminary results of experiments, KAB 65-8, internal report from ASEA, Västerås (1965) in Swedish.
12. O. NYLUND *et al.*, FRIGG loop project, FRIGG-2, AB Atomenergi, Stockholm, and ASEA, Västerås, Sweden (1968).
13. H. CHRISTENSEN, Power-to-void transfer function, ANL-6385 (1961).
14. R. A. EGEN, D. A. DINGEE and J. W. CHASTAIN, Vapour formation and behaviour in boiling heat transfer, BMI-1163 (1957).

APPENDIX

Investigation of the Effects of Various Parameters on the Rate of Bubble Condensation

The theoretical derivations for calculating the steam volume fraction according to this model were first worked out without any knowledge of the magnitude of the condensation parameter k_c. This analysis was then applied to the experimental data of [10] to calculate k_c and its variations with different parameters such as G, p and q/A. The reasons for using the data of [10] were firstly the possibility of systematically studying the effect of each parameter separately with all other conditions being unchanged and secondly for the relatively good degree of accuracy in those experiments.

In these calculations we used the experimental values of α along with the other parameters to obtain k_c from equations (6)–(10). The variations of k_c with each parameter displayed a certain trend. In the case of G and q/A one could easily approximate the trends by a linear and inversed square root dependence respectively. The proportionality between mass

velocity and Reynolds number suggested the possibility of using the latter dimensionless number. In the case of heat flux dependence we decided to include the physical properties which could influence the rate of bubble production and combined them with q/A in a manner that gave the dimensionless group N_q as expressed in equation (14)—although the significance of such a grouping may be questionable.

Finally, the variation of k_c with pressure was studied by plotting $k_c \cdot (N_q^{\frac{1}{2}}/Re_l)$ as a function of pressure. This curve was then compared with various combinations of the physical properties of steam and water. A good agreement was found between this curve and the combination given in equation (15) which also had the right physical dimensions. The effect of Prandtl's number is not clearly established. This is due to the fact that the reference data are from experiments with heavy water and for this substance Prandtl's number happens to be almost constant within the covered range of pressure variations.

An entirely different approach in correlating k_c with the significant parameters would be to express it as

$$k_c = \frac{G}{\sqrt{q/A}} \cdot f_g \cdot \frac{\alpha^{\frac{1}{4}}}{1-\alpha} \cdot f(p) \qquad (A.1)$$

in which f_g should represent the geometry dependent function and $f(p)$ the pressure dependence as a whole. This analysis was actually followed and for the data of [10] we found

$$f(p) = -8{\cdot}3 \times 10^5 + 1{\cdot}340\, p - \frac{4860}{0{\cdot}000918 + \dfrac{10^{10}}{p^2}} \qquad (A.2)$$

where p is pressure in N/m^2 and $f(p)$ has the dimensions of

$$\mathrm{kg}^{\frac{1}{4}}/(m^2 \cdot \mathrm{s}^{1{\cdot}5} {}^{\circ}\mathrm{C}) \ .$$

The pressure dependent function was obtained from heavy water data and when used for comparison with data from light water experiments, it gave almost the same level of deviations as when we used the non-dimensional groups appearing in equations (14)–(16). We then decided to use the first approach.

It is plausible that better ways of expressing the dependence of the condensation coefficient on the physical properties of the liquid and vapour may be obtained. A study on this subject requires some data from boiling substances other than than D_2O and H_2O and with considerably different physical properties.

CALCUL DE LA FRACTION VOLUMIQUE DE VIDES DANS LES REGIONS D'EBULLITION SOUS-REFROIDIE ET DE QUALITE

Résumé—Le problème complexe du calcul des vides, dans les différentes régions de l'écoulement dû à l'ébullition est divisé en deux parties.

La première partie comprend seulement la description des mécanismes et la calcul des vitesses de transport de chaleur pour la vapeur et le liquide. On suppose que la chaleur est enlevée par la production de vapeur, le chauffage du liquide qui remplace les bulles détachées, et en certains endroits, par le transport de chaleur monophasique. En considérant la vitesse de condensation de la vapeur en liquide, on obtient une équation pour les changements différentiels dans la vraie qualité de vapeur d'un bout à l'autre des régions d'ébullition. L'intégration de cette équation fournit la fraction pondérale de la vapeur à n'importe quelle position.

La seconde partie du problème concerne la détermination des fractions de vide correspondant aux qualités de vapeur calculées. Dans ce but, nous employons les dérivations de Zuber et Findlay [9].

Ce modèle est comparé avec les résultats de différentes géométries y compris les petits canaux rectangulaires et les grands faisceaux de barres. Les résultats englobent les pressions de 19 à 138 bars, les flux de chaleur de 18 à 120 W/cm^2 avec beaucoup de sousrefroidissements différents et de vitesses massiques. L'accord est généralement très bon.

BERECHNUNG DES DAMPFVOLUMENANTEILS IM BEREICH DES UNTERKÜHLTEN SIEDENS UND BEIM SIEDEN IM QUALITÄTSBEREICHT.

Zusammenfassung— Das verwickelte Problem der Berechnung des Dampfvolumenanteils in den verschiedenen Bereichen des Siedens wird in zwei Abschnitte unterteilt.

Der erste Teil schliesst nur die Beschreibung der Mechanismen und die Berechnung des Wärmeüberganges für Dampf und Flüssigkeit ein. Es wird angenommen, dass die Wärme durch die Erzeugung von Dampf, Auflösung der Flüssigkeit, welche die angelösten Blasen ersetzt, und in einigen Fällen durch Einphasen-Wärmeübergang wegtransportiert wird. Durch Betrachtung der in der Flüssigkeit kondensierenden Dampfmengen erhält man eine Gleichung für die differentiellen Änderungen der tatsächlichen Dampfqualität innerhalb der Siedebereiche. Die Integration dieser Gleichung ergibt den Dampfgewichtsanteil für jede Position.

Der zweite Teil des Problems führt zur Bestimmung der den Dampfqualitäten entsprechenden Dampfvolumenanteilen. Zu diesem Zweck wurden Ableitungen von Zuber und Findlay [9] verwendet.

Dieses Modell wird mit Messdaten für verschiedene Geometrien, einschliesslich schmaler rechteckiger Kanäle und umfangreicher Stabbündel, verglichen. Die Daten überdecken eine Messbereich für Drücke von 19 bis 138 bar, Heizflächenbelastungen von 18 bis 120 W/cm^2 sowie viele verschiedene Unterkühlungen und Mengenstromdichten.

Die Übereinstimmung ist im allgemeinen sehr gut.

РАСЧЕТ КОНЦЕНТРАЦИИ ПАРА ПРИ КИПЕНИИ В ОБЛАСТИ НЕДОГРЕВА И ПЕРЕГРЕВА

Аннотация—Сложная задача расчета концентрации пара в различных областях потока при кипении разбита на две части.

В первой части описываются механизмы и расчет интенсивности теплообмена пара и жидкости. Предполагается, что тепло переносится генерацией пара, нагреванием жидкости, которая заменяет оторванные пузырьки, а в некоторых частях однофазным теплообменом. С учетом скорости конденсации пара в жидкости получено уравнение для различных изменений истинного паросодержания в областях кипения. Интегрирование этого уравнкния дает весовое содержание пара в любой точке.

Во второй части определяются концентрации пара, соответствующие расчетным значениям сухости пара. Для этого использовались выводы зубера и финдлея (9).

Эта модель сравнивается с моделями различных конфигураций, включая небольшие прямоугольные каналы и большие пучки стержней. В этих данных давление изменялось от 19 до 138 бар, тепловые потоки от 18 до 120 ватт/см^2 при различных значениях недогрева и массовых скоростях. Получено очень хорошее соответствие данных.